Photo by Alexander Andrews on Unsplash

On microlensing of axion clumps

PRD 104 (2021) 123012 - JCAP 01 (2018) 037

Enrico D. Schiappacasse
University of Jyvaskyla & University of Helsinki (HIP)

Dark sectors of astroparticle physics
ASTRO-DARK 2021 (7-10 December)

University of Jyvaskyla &
University of Helsinki (HIP)

With the collaboration of Kohei Fujikura (RESCEU), Mark Hertzberg (Tufts U.) , Masahide Yamaguchi (TiTech)

QCD-Axion in a nutshell

- A wide range of astrophysical observations are well explained by including cold dark matter (CDM) (Peebles, 2015).

- A popular dark matter candidate is the QCD axion: PG-boson associated with SSB of $U(1)_{PQ}$, which was introduced as a possible solution of the strong CP problem (Peccei and Quinn, 1977) .

- The axion field acquires a mass after the QCD phase transition, and then begin to act as a form of CDM (Preskill et al. 1983).

- Extensively axion searching

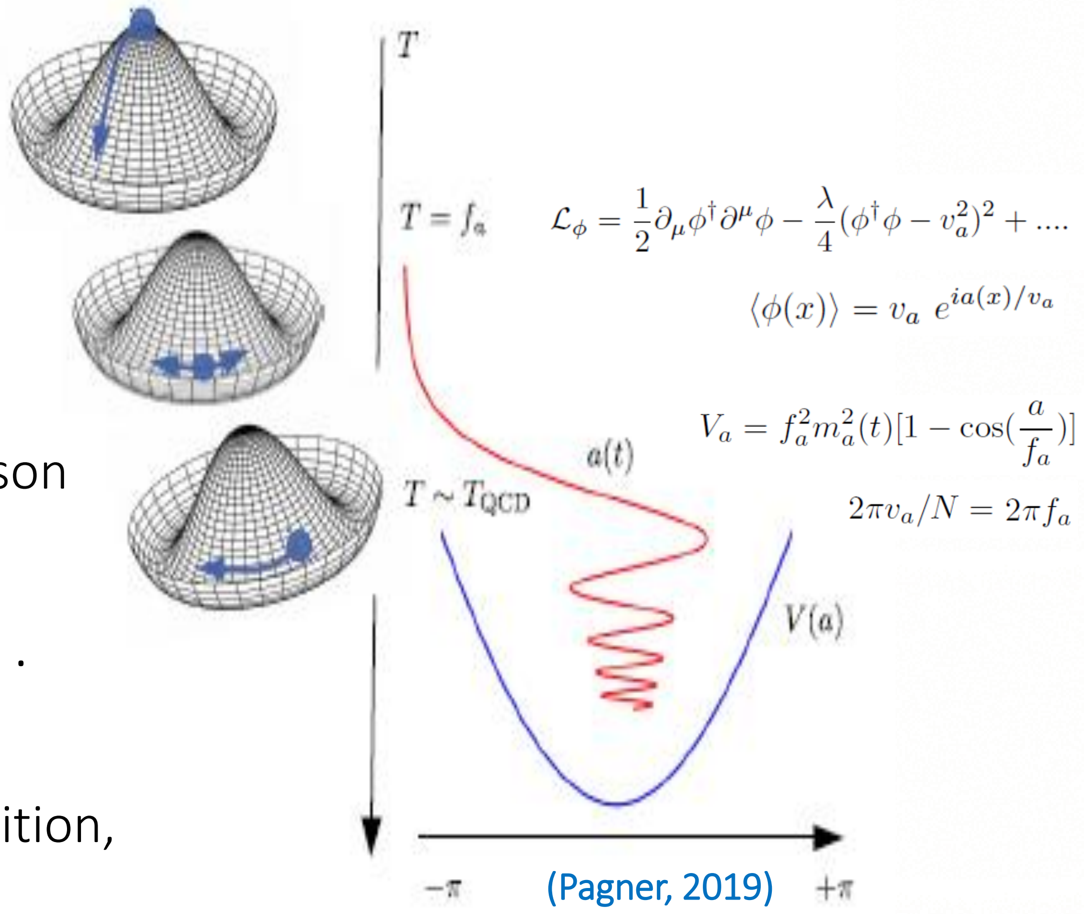

(Pagner, 2019)

- Ground based experiments as ADMX (Asztalo et al. 2010)
- FRB and axion miniclusters (Tkachev 2015)
- Transient radio emission from axion photon conversion during neutron star-ultracompact minihalo encounters (Nurmi, Schiappacasse, Yanagida, 2021)

DARK MATTER AXION CLUMPS

- We are interested in BEC of axions:

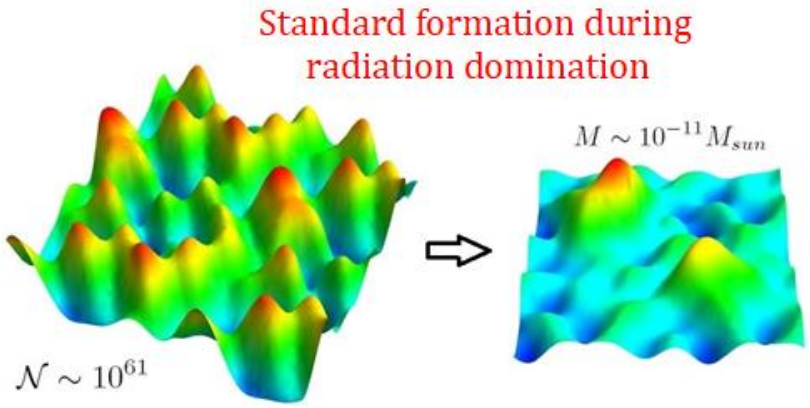

(Sikivie and Yang, 2009)

On small scales axions can gravitationally thermalize leading to a type of BEC

Condensate of short range order driven by attractive interactions : gravity + self interactions λa^4

(Guth, Hertzberg, and Prescod-Weinstein, 2015)

- In the effective theory for axions, they can be described by a real scalar field $\phi(x,t)$ with a small potential $V(a)$ coming from nonperturbative QCD effects.
- Around CP preserving vacuum:
- For the standard QCD axion

$$\mathcal{L} = \sqrt{-g}\left[\frac{R}{16\pi G_N} + g^{\mu\nu}\nabla_\mu a \nabla_\nu a - V(a)\right] \Rightarrow V(a) = \frac{1}{2}m_\phi^2 a^2 + \frac{\lambda}{4!}a^4 + \cdots$$

$$m_a(m_{u,d,\pi}, f_\pi, f_a) \simeq 10^{-5}\text{eV}\left(\frac{6\cdot 10^{11}\text{GeV}}{F_a}\right) \quad \text{and} \quad \lambda = -\gamma\frac{m_a^2}{F_a^2} < 0$$

$\gamma = 1$: $\quad V(a) = m_a^2 F_a^2[1-\cos(a/F_a)]$

$\gamma = 1 - 3m_u m_d/(m_u+m_d)^2 \approx 0.3$ (Grilli et al., 2016)

- In the non-relativistic regime we can rewrite the real axion field in terms of a complex Schrodinger field ψ

$$\phi(\boldsymbol{x},t)=\frac{1}{\sqrt{2m_a}}\left[e^{-im_a t}\psi(\boldsymbol{x},t)+e^{im_a t}\psi^*(\boldsymbol{x},t)\right]$$

- The dynamics of ψ is given by the standard non-relativistic Hamiltonian:

($\dot{\psi}(\boldsymbol{x},t)\ll m_a\psi(\boldsymbol{x},t)$, dropping high oscillating terms)

$$H_{nr}=H_{kin}+H_{int}+H_{grav}$$

(Guth, Hertzberg, and Prescod-Weinstein, 2015; Schiappacasse and Hertzberg, 2017)

$$H_{kin}=\frac{1}{2m_a}\int d^3x\,\nabla\psi^*\cdot\nabla\psi\,,\qquad H_{int}=\frac{\lambda}{16m_a^2}\int d^3x\psi^{*2}\psi^2,$$

$$H_{grav}=-\frac{Gm_a^2}{2}\int d^3x\int d^3x'\,\frac{\psi^*(\boldsymbol{x})\psi^*(\boldsymbol{x}')\psi(\boldsymbol{x})\psi(\boldsymbol{x}')}{|\boldsymbol{x}-\boldsymbol{x}'|}$$

- H_{nr} carries a global $\mathrm{U}(1)$ symmetry $\psi\to\psi e^{i\theta}$ associated with a conserved particle number

$$N=\int d^3x\,\psi^*(\boldsymbol{x})\psi(\boldsymbol{x})$$

BEC : State of minimum energy at fixed N (spherically symmetry)

SPHERICALLY SYMMETRIC CLUMP CONDENSATES

$\Psi(r)$ describes the radial profile
μ describes the correction to the frequency

- Gravity will inevitably cause a homogeneous condensate to fragment into an inhomogeneous field configuration: locally this leads to the formation of BEC clumps.
- The true BEC ground state is guaranteed to be spherically symmetric: $\psi(r,t) = \Psi(r)e^{-i\mu t}$
- The time independent field equation for a spherically symmetric eigenstate is

$$V_{nr} = -\frac{\Psi^4}{16{F_a}^2}$$

$$\mu\Psi = -\frac{1}{2m}\left(\Psi'' + \frac{2}{r}\Psi'\right) - 4\pi G m_a^2 \Psi \int_0^\infty dr' r'^2 \, \frac{\Psi(r')^2}{r_>} + \frac{1}{2}\frac{\partial V_{nr}}{\partial \Psi}$$

(Schiappacasse and Hertzberg, 2017)

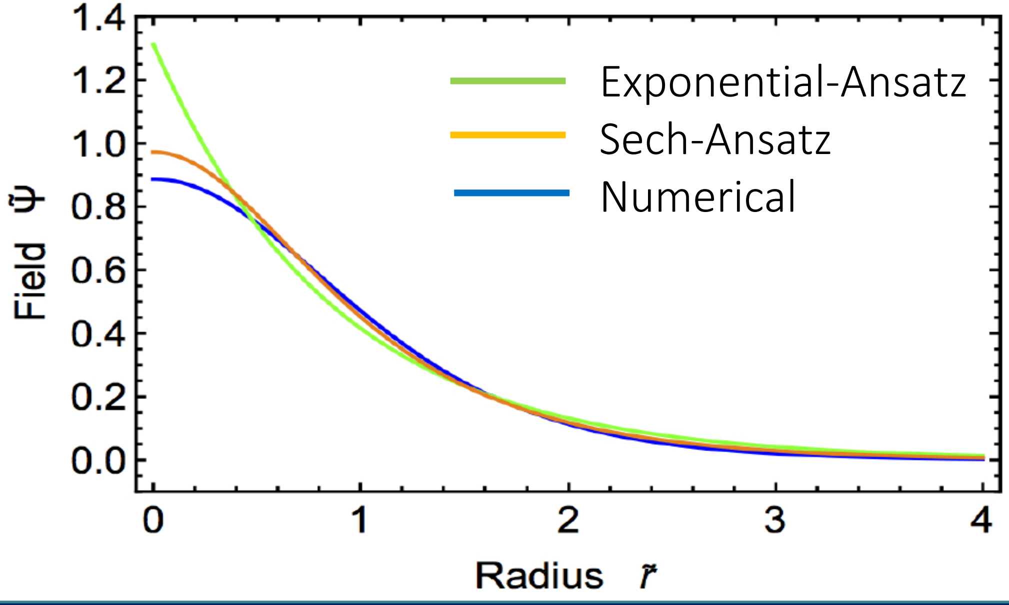

Far field region ($r \to \infty$) : Identical to the structure of the time independent Schrödinger equation for the hydrogen atom under replacement Gm^2N→ e^2

Near field region ($r \to 0$) : Corrections from self-interactions become important. There are no know full analytic solutions.

SPHERICALLY SYMMETRIC CLUMP CONDENSATES

- $\frac{d\tilde{H}}{d\tilde{R}} = 0$ to obtain conditions for stationary solutions
- For any $(\tilde{a}, \tilde{b}, \tilde{c})$ there ate two branches of solutions

Exponential-Linear Anstaz

$$\Psi(r) = \sqrt{\frac{N}{7\pi R^3}}\left(1 + \frac{r}{R}\right)e^{-r/R}$$

Scale length
(variational parameter)

$$\tilde{R} = \frac{a \pm \sqrt{a^2 - 3bc\tilde{N}^2}}{b\tilde{N}}$$

$$\tilde{H}_{\rm tot} = a\frac{\tilde{N}}{\tilde{R}^2} - b\frac{\tilde{N}^2}{\tilde{R}} - c\frac{\tilde{N}^2}{\tilde{R}^3}$$

Any localized anstaz of a single parameter R

State of minimum energy at fixed $\tilde{N}$
(spherically symmetry)

$$\mathrm{N} = 4\pi \int_0^\infty |\psi(r,t)|^2\, r^2 dr$$

$$\widetilde{N} \equiv \frac{m_a^2\sqrt{G_N}}{F_a}N$$

$$\tilde{R} = m_a\sqrt{G_N}F_a R$$

$$\widetilde{H}_{\rm tot} \equiv \frac{m_a}{F_a^3\sqrt{G_N}}H_{\rm tot}$$

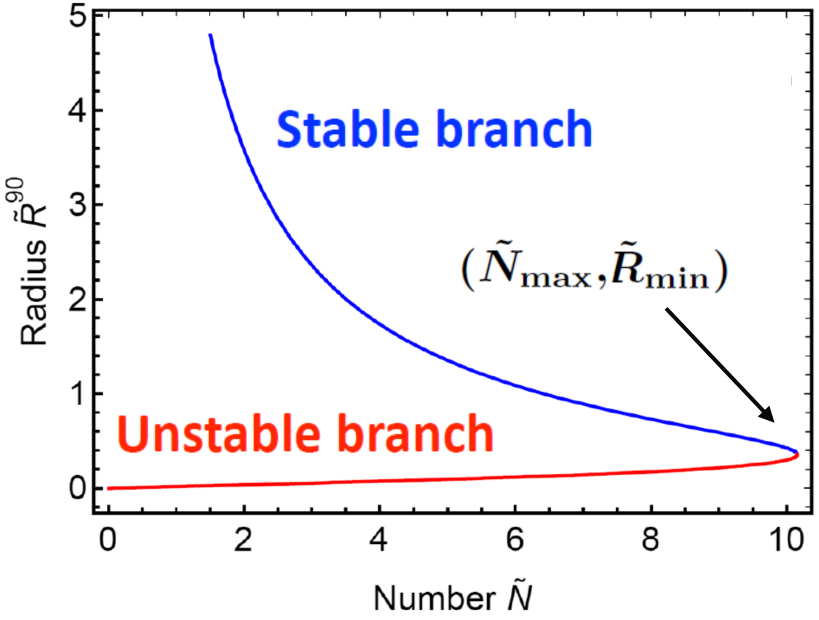

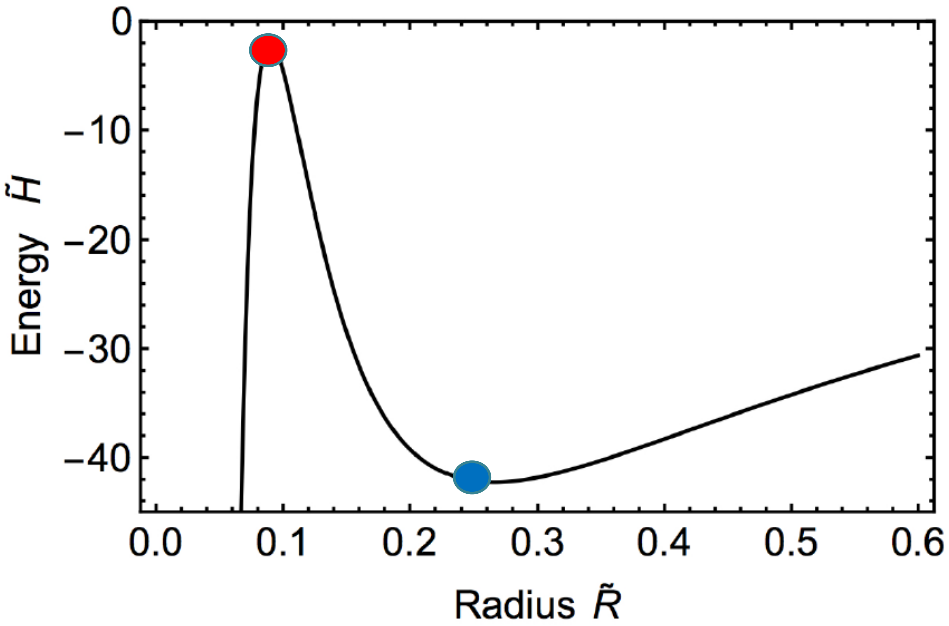

SPHERICALLY SYMMETRIC CLUMP CONDENSATES

- We compute the maximum mass, and the minimum clump size for axion clumps as follows:

$$M_{max} \sim 1.2\ \times 10^{-11}\, M_{\odot} \left(\frac{10^{-5}\mathrm{eV}}{m_a}\right) \left(\frac{F_a}{6 \cdot 10^{11}\mathrm{GeV}}\right) \left(\frac{\gamma}{0.3}\right)^{1/2}$$

$$R_{min} \sim 22\ \mathrm{km} \left(\frac{10^{-5}\mathrm{eV}}{m_a}\right) \left(\frac{6 \cdot 10^{11}\mathrm{GeV}}{F_a}\right) \left(\frac{0.3}{\gamma}\right)^{1/2}$$

- A simple manipulation allows us to express (M_{clump}, R) of any clump as

$$M_{clump}(R) = \alpha M_{max}(R_{min})$$

$$R = \left(\frac{1+\sqrt{1-\alpha^2}}{\alpha}\right) R_{min}$$

$$\boldsymbol{\alpha \in [0, 1]}$$

Gravitational Microlensing (PBHs)

- The image of a background star is distorted when a massive compact object passes close to its line-of-sight. The time varying amplification of the brightness of the source star is called a microlensing event.
- Massive compact objects can be constrained by using the microlensing events reported from different surveys. Subaru HSC & EROS-2 surveys

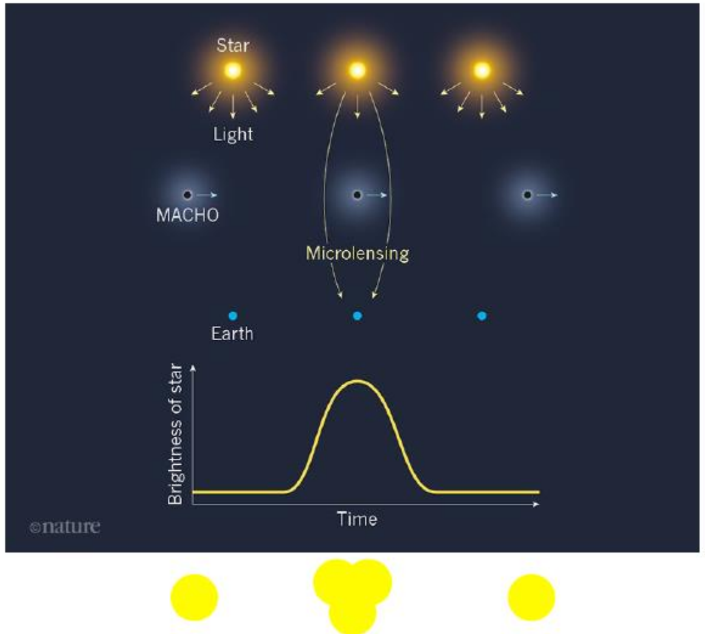

$$\beta = \theta - \frac{D_{\rm LS}}{D_{\rm L} D_{\rm S}} \frac{4 G_N M}{\theta}$$

Pointlike Einstein ring angle is a solution of $\beta(\theta_E) = 0$

$$\theta_E = \sqrt{4 G_N M \frac{D_{\rm LS}}{D_{\rm S} D_{\rm L}}}$$

$$u = t - \frac{1}{t}, \quad \text{where } u = \beta/\theta_E \text{ and } t_i = \theta_i/\theta_E.$$ Lens Equation

$$\mu_i \equiv \frac{\theta_i}{\beta}\frac{d\theta_i}{d\beta} = \frac{t_i}{u}\frac{dt_i}{du}, \qquad \mu_{\rm tot}(\boldsymbol{u_T}) = |\mu_1| + |\mu_2| \geq 1.34$$ Magnification

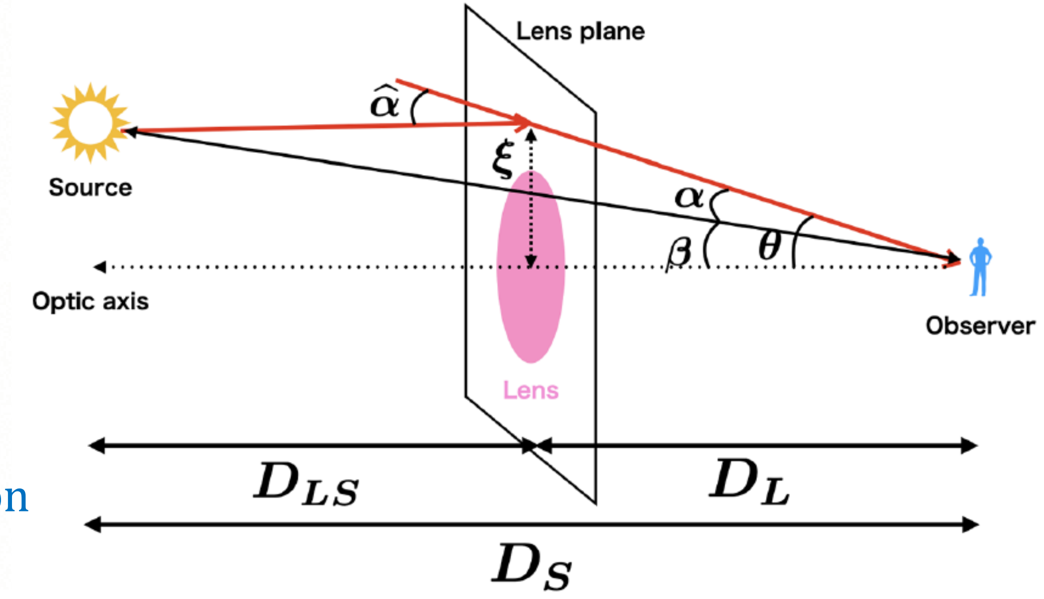

- It is assumed that microlensing events follows a Poisson distribution

- Probability of observing N_{obs} microlensing events:

$$P(N_{\rm obs}, N_{\rm exp}) = (N_{\rm exp})^{N_{\rm obs}} e^{-N_{\rm exp}} / N_{\rm obs}!$$

$N_{\rm exp}$ **: Expected number of events**

$N_{\rm obs}$ **: Observed microlensing events**

If $N_{\rm obs} = 0\ (1)$, $N_{\rm exp} > 3\ (4.74)$ is excluded at 95% confidence level.

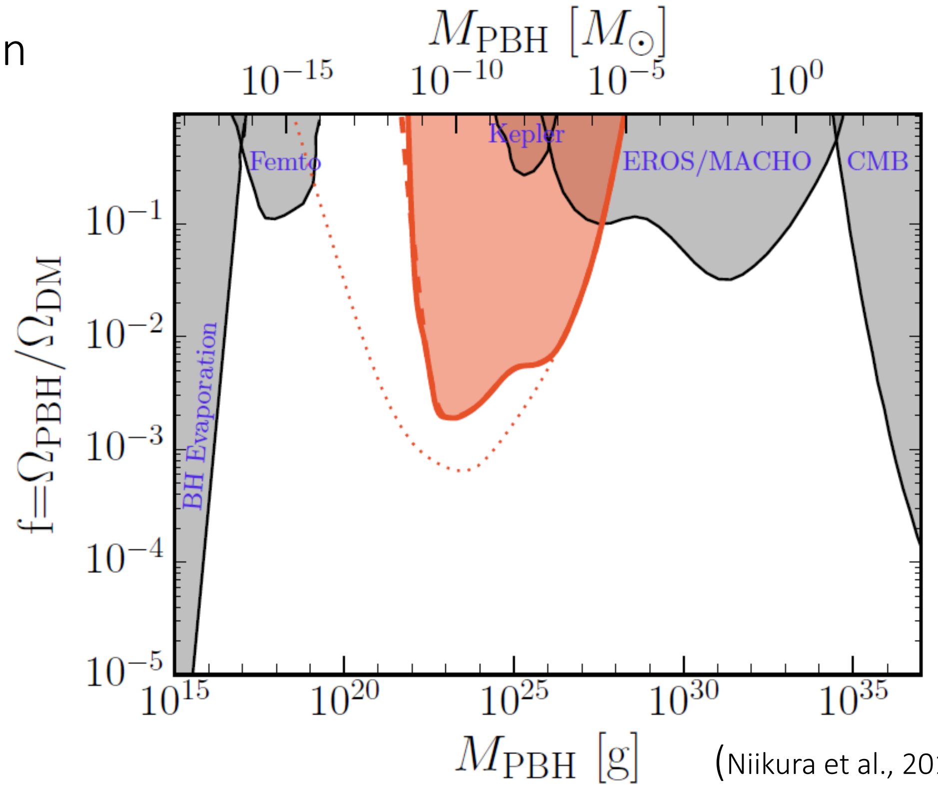

(Niikura et al., 2017)

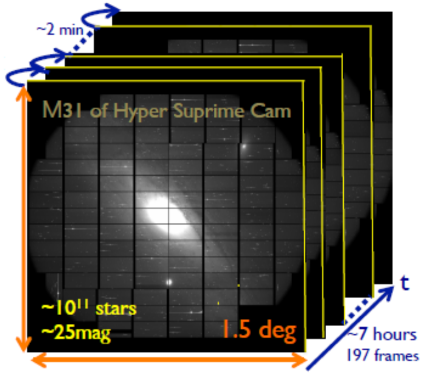

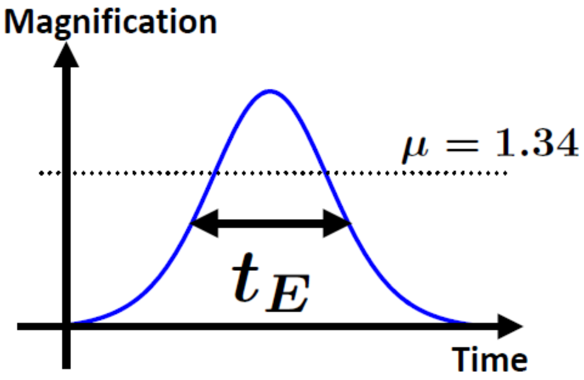

Subaru Hyper Suprime-Cam

$2\,{\rm min} < t_E < 7\,{\rm hr}$

$7\,{\rm hr} \Rightarrow M_{\rm PBH} \sim 10^{-5} M_\odot$

$$t_E \sim R_E/v \sim 10\,{\rm min} \left(\frac{M_{\rm PBH}}{10^{-8} M_\odot}\right)^{\frac{1}{2}} \left(\frac{d}{100\,{\rm kpc}}\right)^{\frac{1}{2}} \left(\frac{v}{200\,{\rm km/s}}\right)^{-1}$$

We can theoretically calculate $N_{\rm exp}$ given dark matter model.

$$N_{\rm exp} = N_{\rm exp}(u_T, M_{\rm clump}, \rho_{\rm DM}, f_{\rm DM}(v), T_{\rm obs})$$

Gravitational Microlensing of Axion Clumps

We solve lens equation including finite lens and source size effects!

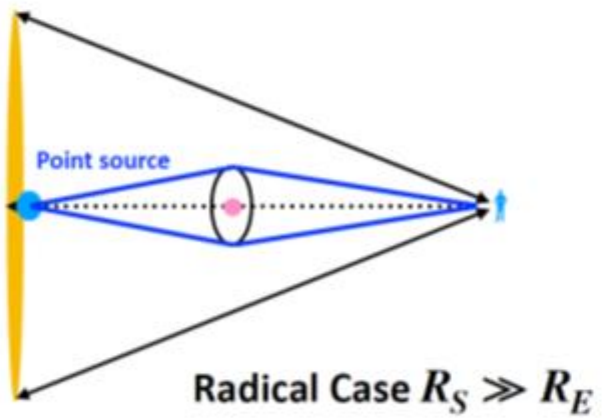

(Diagrams made by K. Fujikura)

$$M_{\mathrm{PBH}} \to M_{\mathrm{clump}}(m_a, F_a, \alpha)$$

$$\Omega_{\mathrm{PBH}}/\Omega_{\mathrm{DM}} \to \Omega_{\mathrm{clump}}/\Omega_{\mathrm{DM}}$$

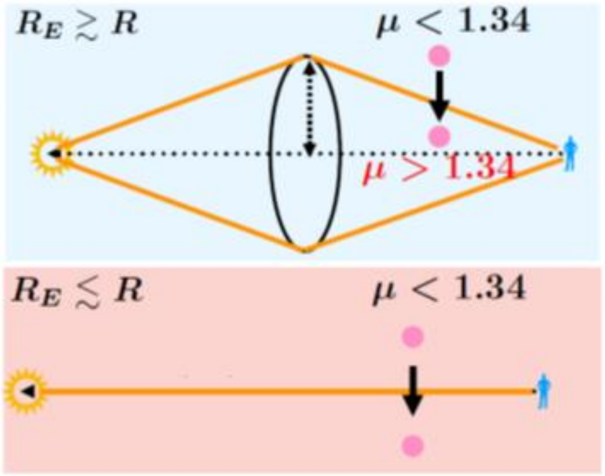

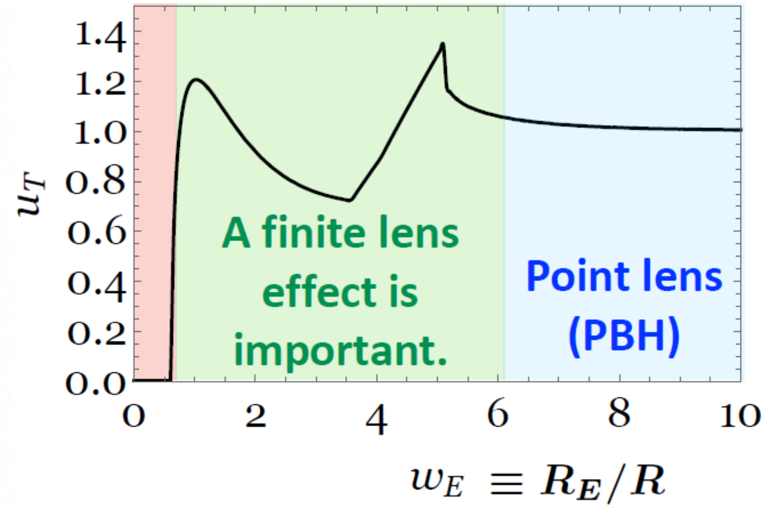

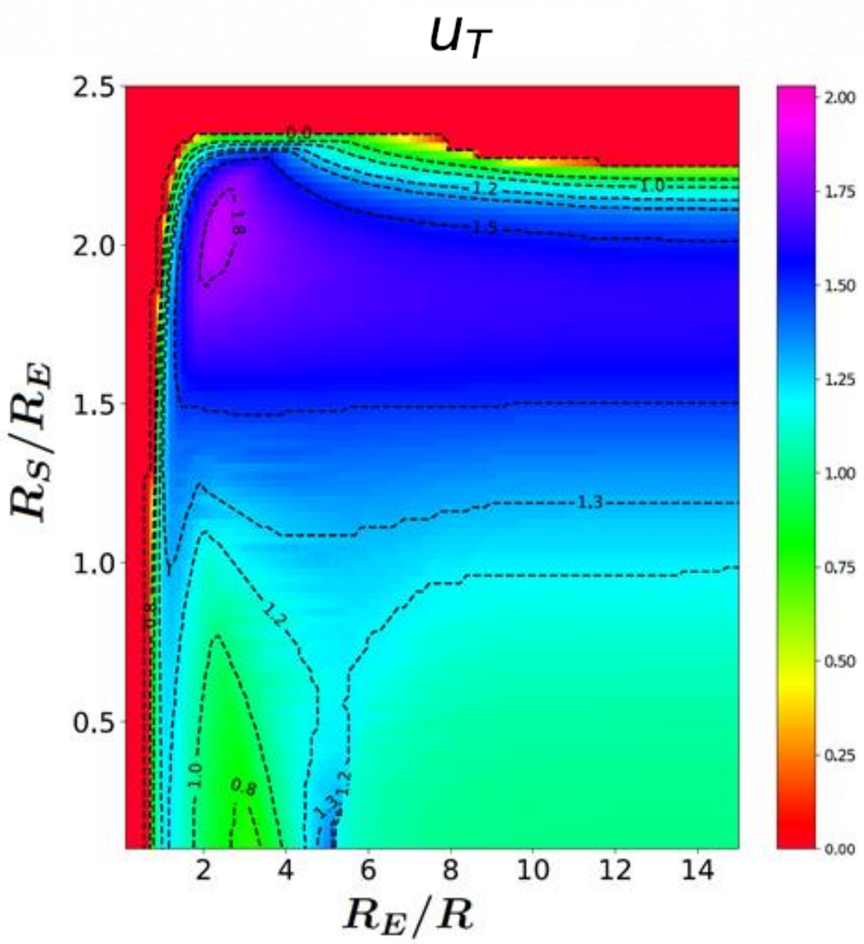

No microlensing events for $R_E < 0.6 \times R$.
(A finite lens size effect)

No microlensing events for $R_S > 2.3 \times R_E$.
(A finite source size effect)

CONSTRAINTS FOR AXION CLUMPS

SUBARU HSC (2 min, 7 hr)

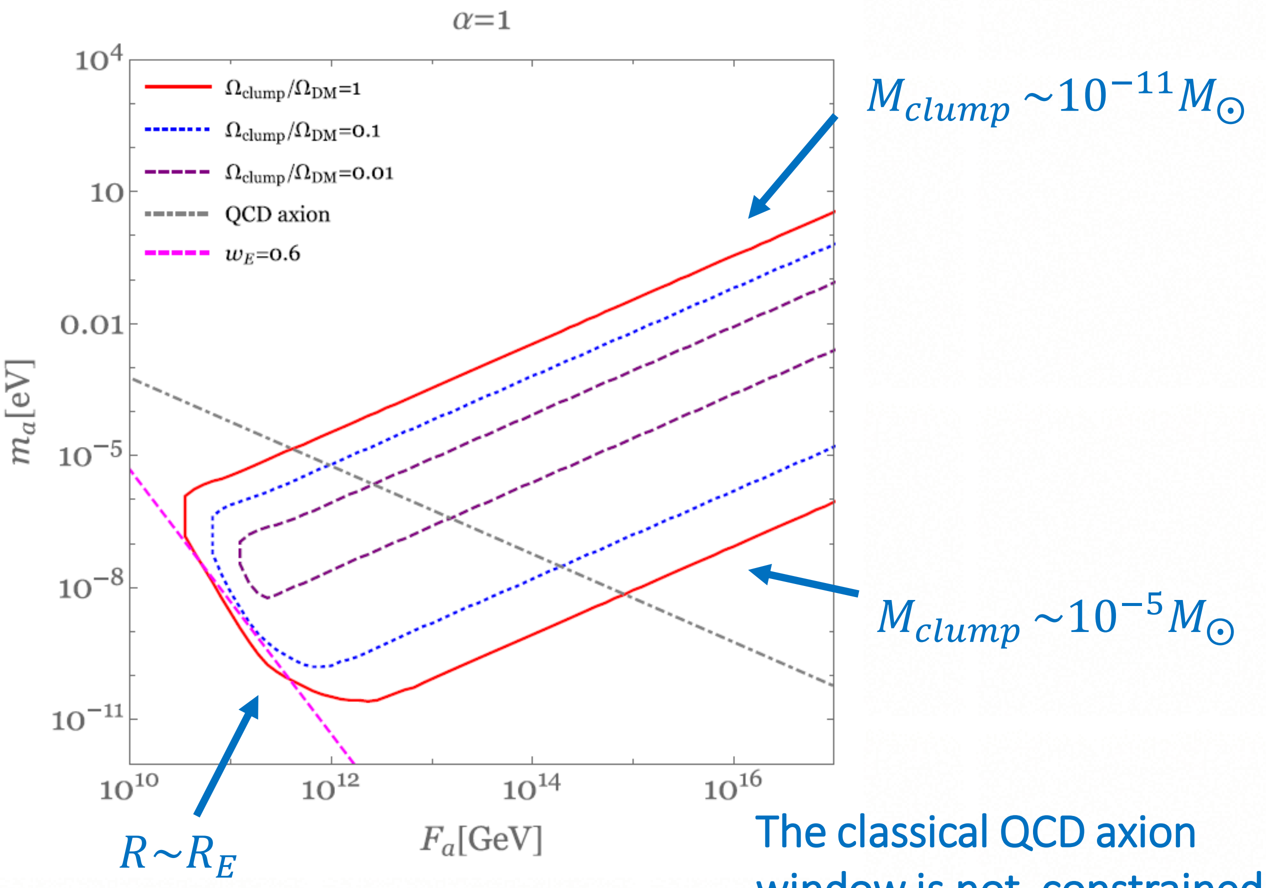

The classical QCD axion window is not constrained due to a finite source size effect.

EROS-2 (1 day, 250 day)

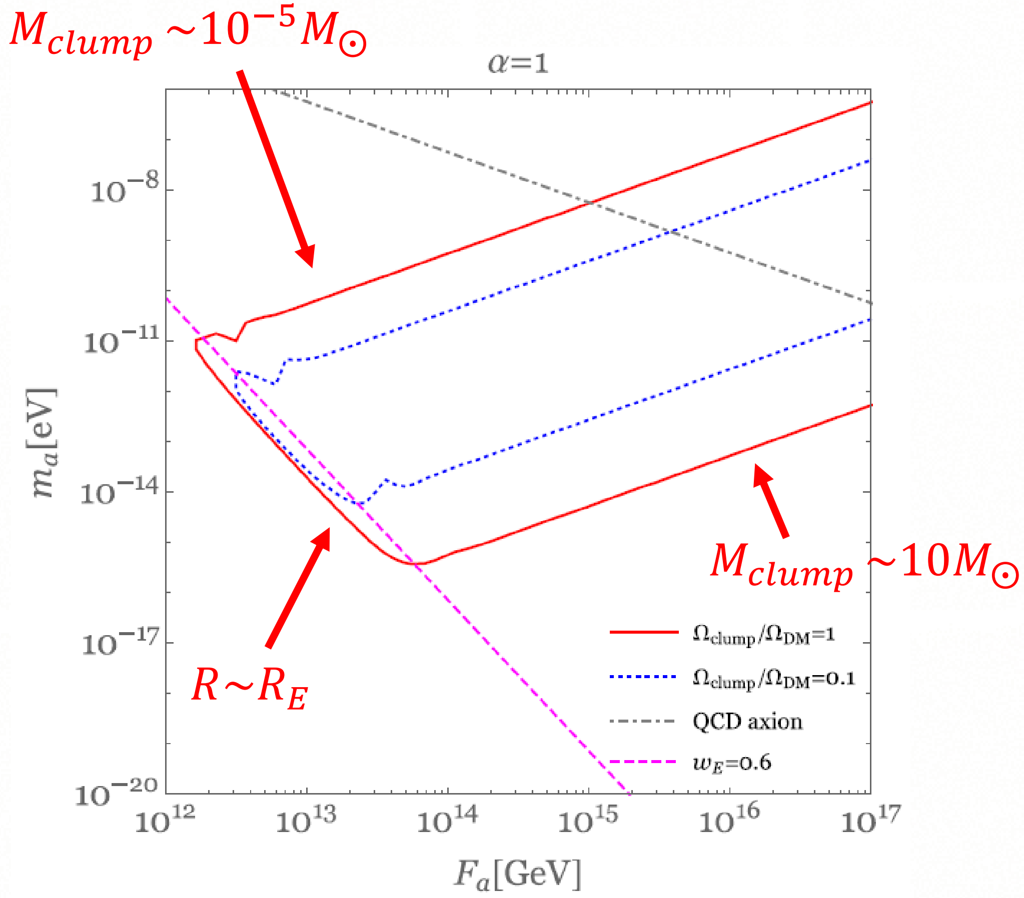

$\boldsymbol{f_a > 10^{15}}$**GeV** can be constrained for the QCD axion

SUBARU HSC

Finite source size effect

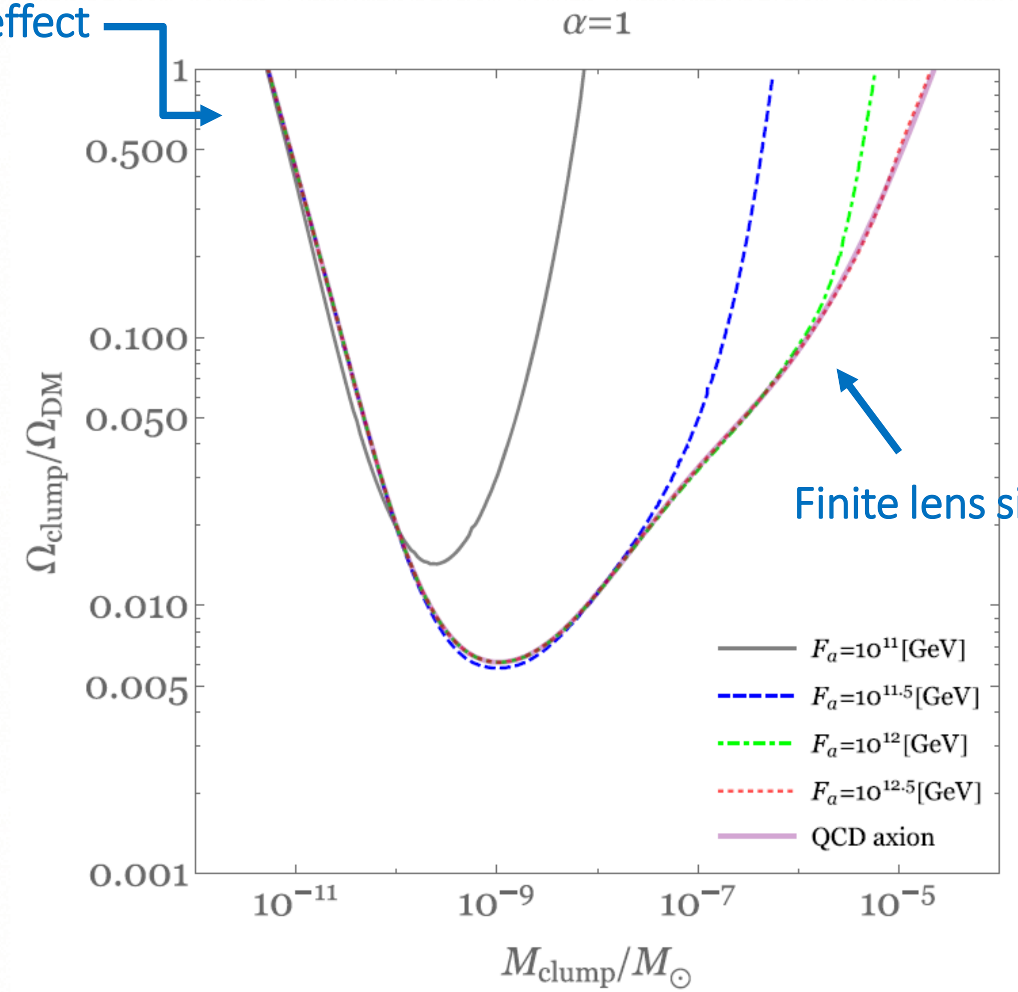

Finite lens size effect

For $M_{clump} < 10^{-8} M_\odot$, we have $R_E \sim R_\odot$

EROS-2

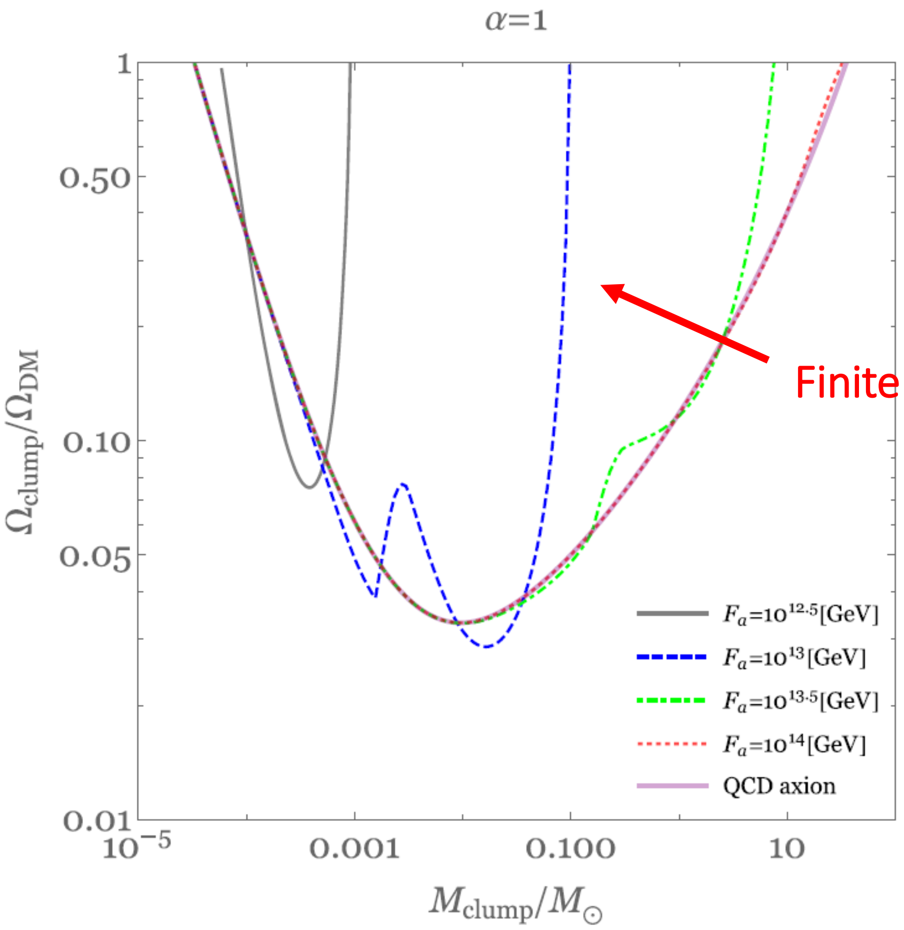

Finite lens size effect

$$R_E \simeq 1.9 \times 10^3 \times R_\odot \left(\frac{M_{\rm clump}}{M_\odot}\right)^{\frac{1}{2}} \times \left(\frac{D_S}{10\ {\rm kpc}}\right)^{\frac{1}{2}}$$

$$w_E \simeq 10^2 \times \left(\frac{m_a}{10^{-5}\ {\rm eV}}\right)^{\frac{1}{2}} \left(\frac{F_a}{10^{12}\ {\rm GeV}}\right)^{\frac{3}{2}} \times \left(\frac{\gamma}{0.3}\right)^{\frac{3}{4}} \left(\frac{D_S}{10\ {\rm kpc}}\right)^{\frac{1}{2}} \left(\frac{\alpha^{\frac{3}{2}}}{1+\sqrt{1-\alpha^2}}\right)$$

CONCLUSIONS

- We give for the first time microlensing constraints from the EROS-2 and Subaru HSC surveys on QCD axion (axion-like) dark matter clumps including finite lens and source size effects.

- We found that the brightness magnification of the source stars is shut-off for the finite lens and source size effects when $(R_E < 0.6R)$ and $(R_s > 2.3R_E)$, respectively.

- EROS-2 and Subaru HSC surveys are able to constrain axion clumps within the mass regime $10^{-5} \lesssim M_{clump}/M_\odot \lesssim 10$ and $10^{-11} \lesssim M_{clump}/M_\odot \lesssim 10^{-5}$, respectively.

- For the QCD axion, only the high breaking scale regime $F_a \gtrsim 10^{12}\mathrm{GeV}$ can be constrained due to the sizeable finite source size effect present in the regime at which the axion decay is within the classical QCD axion window.

SOME REFERENCES

- K. Fujikura, M. P. Hertzberg, E. D. Schiappacasse, M. Yamaguchi, "Microlensing constraints on axion stars including finite lens and source size effects" PRD **104**, 123012 (2021).
- E. D. Schiappacasse and M. P. Hertzberg, "Analysis of Dark Matter Axion Clumps with Spherical Symmetry," JCAP **1801**, 037 (2018).
- M. P. Hertzberg and E. D. Schiappacasse, "Scalar Dark Matter Clumps with Angular Momentum," arXiv:1804.07255 [hep-ph] (2018).
- A. H. Guth, M. P. Hertzberg and C. Prescod-Weinstein, "Do Dark Matter Axions Form a Condensate with Long-Range Correlation?," Phys. Rev. D **92**, 103513 (2015).
- E. D. Schiappacasse and T. T. Yanagida, "Can QCD axion stars explain Subaru HSC microlensing?," Phys. Rev. D **104**, 103020 (2021).
- J. Preskill, M. B. Wise and F. Wilczek, "Cosmology of the Invisible Axion," Phys. Lett. B **120**, 127 (1983).
- R. D. Peccei and H. R. Quinn, "CP Conservation in the Presence of Instantons," Phys. Rev. Lett. **40,** 279 (1978).
- S. Weinberg, "A New Light Boson?," Phys. Rev. Lett. **40**, 223 (1978).
- J. E. Kim, ''Weak Interaction Singlet and Strong CP Invariance,'' Phys. Rev. Lett. **43**, 103 (1979).
- G. Grilli di Cortana, E. Hardy, J. Pardo Vega and G. Villadoro, "The QCD axion, precisely," JHEP **1601**, 034 (2016).

EROS-2

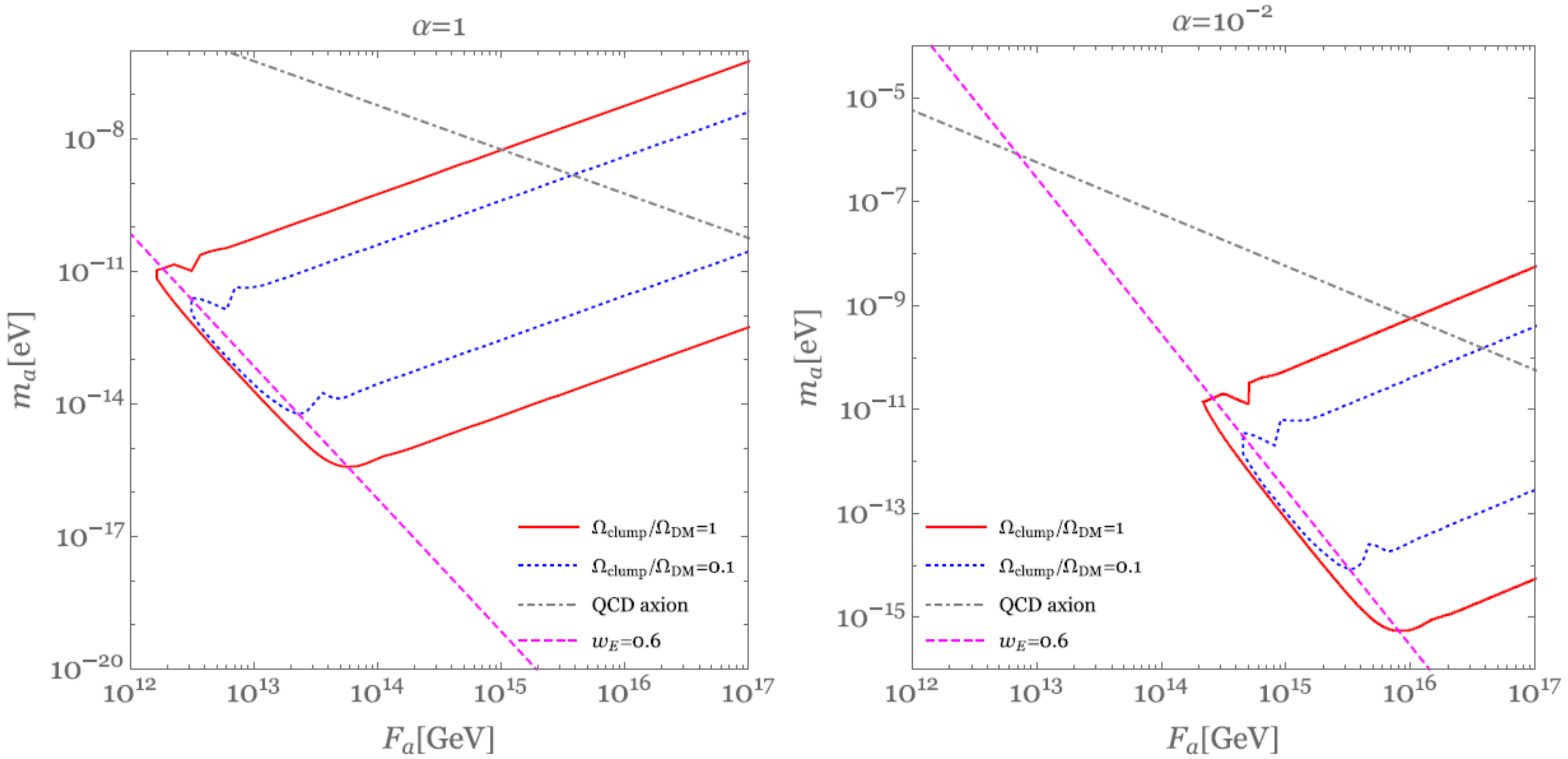

Parameter regions on the (F_a, m_a) plane excluded by the EROS-2 survey are shown for $\Omega_{\rm clump}/\Omega_{\rm DM} = 1$ (red curve) and $\Omega_{\rm clump}/\Omega_{\rm DM} = 0.1$ (blue dotted curve) with $\alpha = 1$ (left) and with $\alpha = 10^{-2}$ (right). The gray colored dotted-dashed contour and magenta colored dashed contour correspond to the parameter of the ordinary QCD axion and $w_E = 0.6$, respectively.

SUBARU HSC

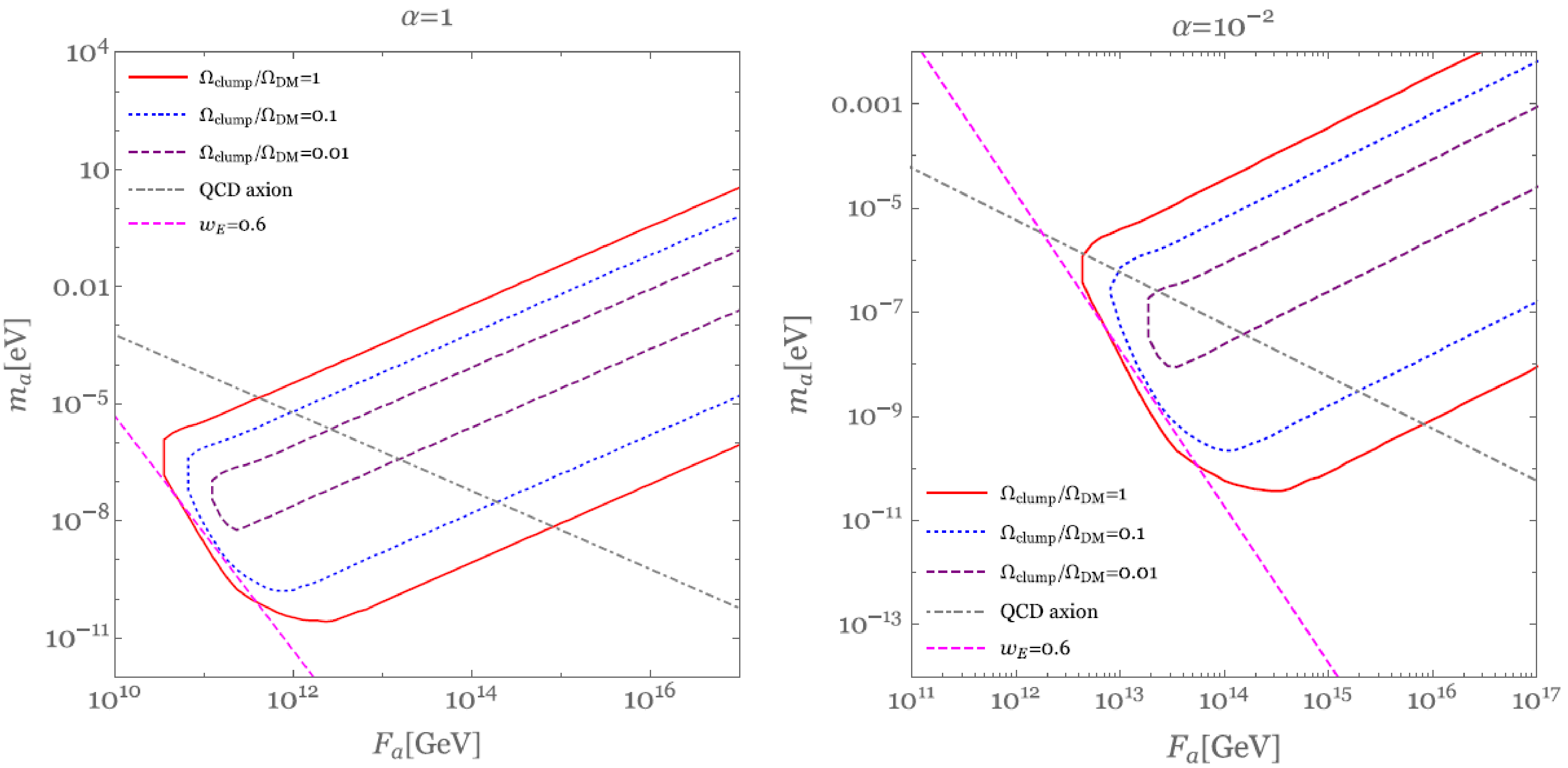

Parameter regions on the (F_a, m_a) plane excluded by the Subaru HSC observation are shown for $\Omega_{\text{clump}}/\Omega_{\text{DM}} = 1$ (red curve), $\Omega_{\text{clump}}/\Omega_{\text{DM}} = 0.1$ (blue dotted curve), and $\Omega_{\text{clump}}/\Omega_{\text{DM}} = 0.01$ (purple dashed curve) with $\alpha = 1$ (left) and with $\alpha = 10^{-2}$ (right). The gray colored dotted-dashed contour and magenta colored dashed contour correspond to the parameter of the ordinary QCD axion and $w_E = 0.6$, respectively.

EROS-2

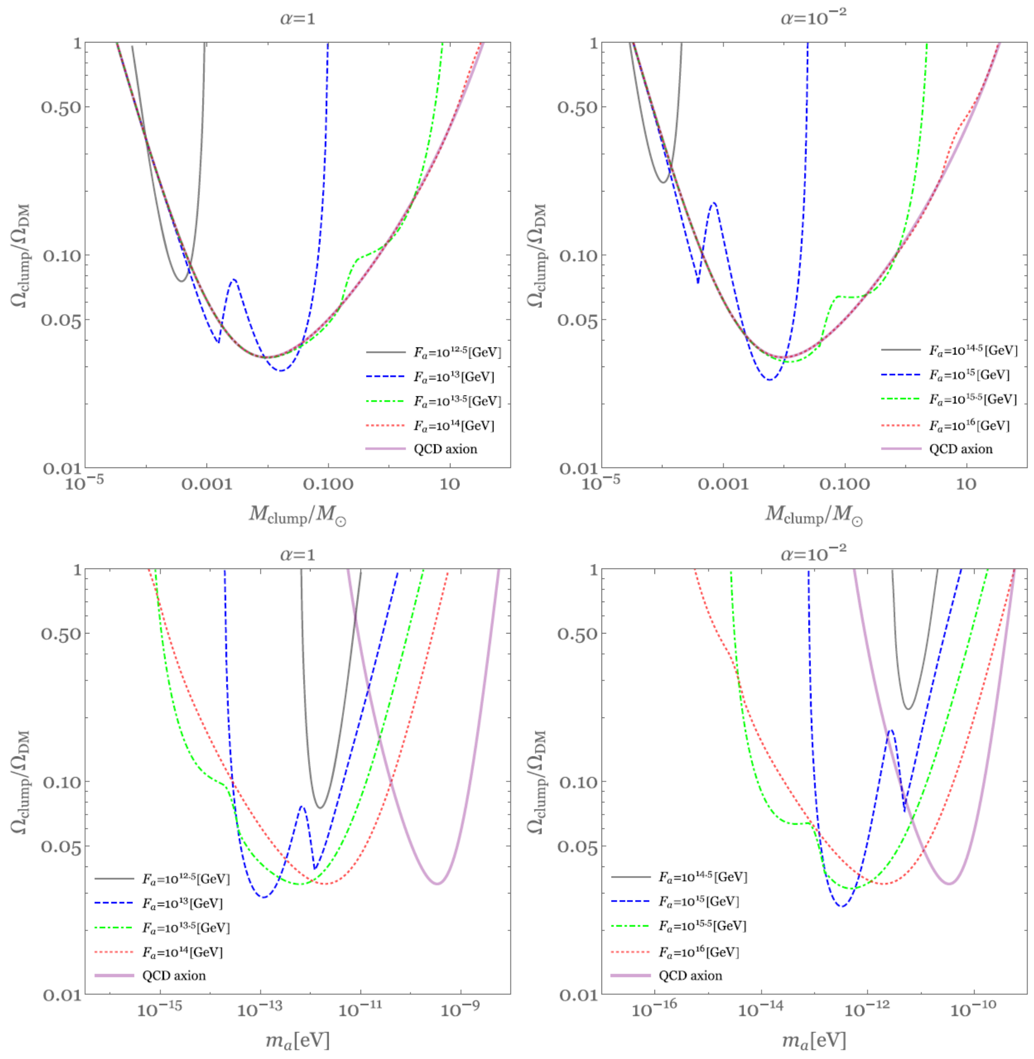

Parameter regions on the $(m_a, \Omega_{\rm clump}/\Omega_{\rm DM})$ plane excluded by the EROS-2 survey are shown with $\alpha = 1$ (upper left) and with $\alpha = 10^{-2}$ (upper right) for the axionlike particles with fixed F_a and for the ordinary QCD axion. Excluded parameter regions on the $(m_a, \Omega_{\rm clump}/\Omega_{\rm DM})$ plane are shown for the same F_a with $\alpha = 1$ (lower left) and with $\alpha = 10^{-2}$ (lower right).

SUBARU HSC

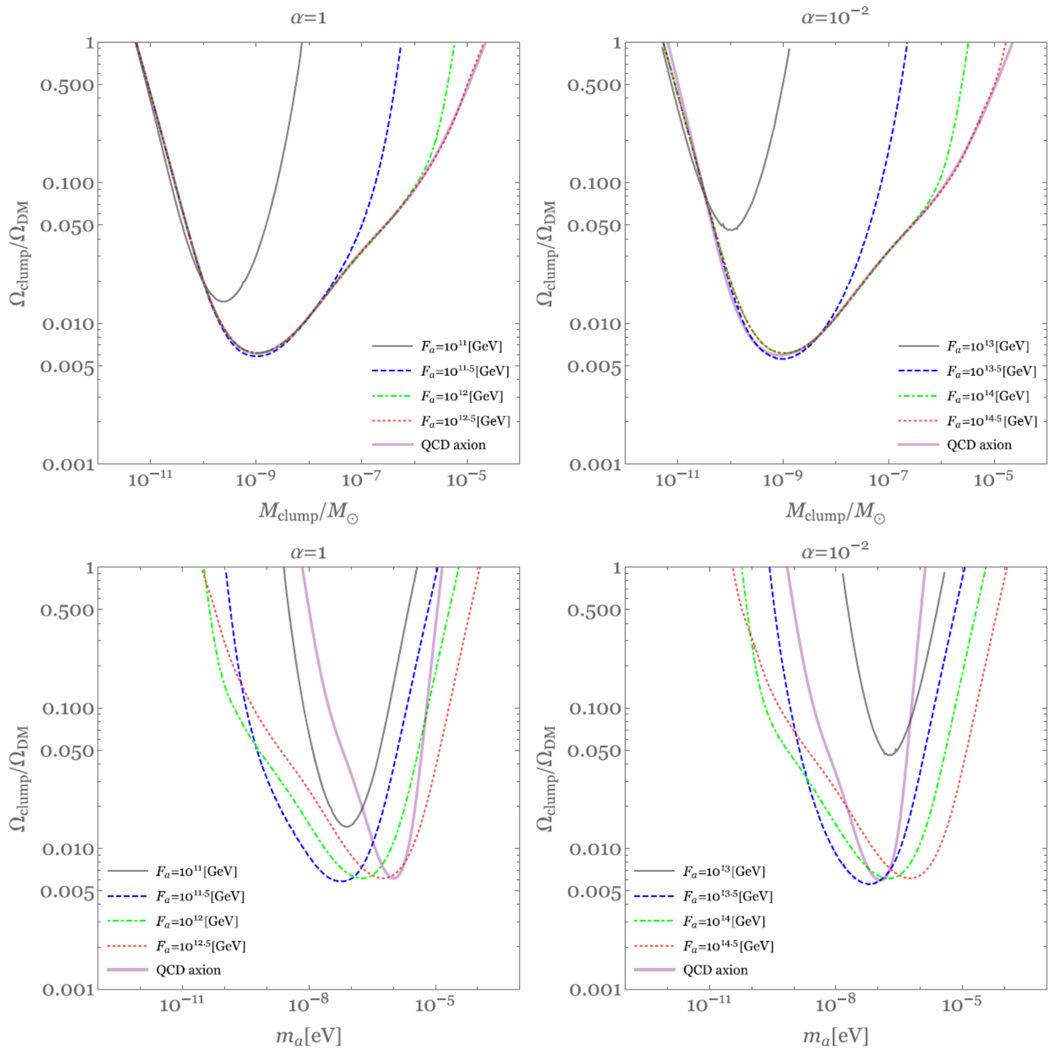

Parameter regions on the $(m_a, \Omega_{\rm clump}/\Omega_{\rm DM})$ plane excluded by the Subaru HSC observation are shown with $\alpha = 1$ (upper left) and with $\alpha = 10^{-2}$ (upper right) for the axionlike particles with several fixed F_a and the ordinary QCD axion. Excluded parameter regions on the $(m_a, \Omega_{\rm clump}/\Omega_{\rm DM})$ plane are shown for the same F_a with $\alpha = 1$ (lower left) and with $\alpha = 10^{-2}$ (lower right).